

Article

Cellulose/Gold Nanocrystal Hybrids via an Ionic Liquid/Aqueous Precipitation Route

Zhonghao Li ^{1,2} and Andreas Taubert ^{1,3,*}

¹ Institute of Chemistry, University of Potsdam, Karl-Liebknecht-Str. 24-25, Building 26, D-14476 Golm, Germany

² Key Laboratory of Liquid Structure and Heredity of Materials, Ministry of Education, School of Materials Science and Engineering, Shandong University, Jinan, Shandong Province 250061, China; E-Mail: zhonghaoli@sdu.edu.cn (Z.L.)

³ Max-Planck-Institute of Colloids and Interfaces, D-14476 Golm, Germany

* Author to whom correspondence should be addressed; E-Mail: ataubert@uni-potsdam.de; Tel.: 0049 (0)331 977 5773; Fax: 0049 0 331 977 5055.

Received: 9 October 2009; in revised form: 12 November 2009 / Accepted: 17 November 2009 / Published: 18 November 2009

Abstract: Injection of a mixture of HAuCl_4 and cellulose dissolved in the ionic liquid (IL) 1-butyl-3-methylimidazolium chloride [Bmim]Cl into aqueous NaBH_4 leads to colloidal gold nanoparticle/cellulose hybrid precipitates. This process is a model example for a very simple and generic approach towards (noble) metal/cellulose hybrids, which could find applications in sensing, sterile filtration, or as biomaterials.

Keywords: cellulose; gold nanoparticles; ionic liquid; precipitation; hybrid material

1. Introduction

Inorganic materials chemistry in ionic liquids (ILs) has recently attracted increasing attention [1–8]. This is because ILs, among other features, enable the synthesis of advanced materials that cannot (easily) be made in conventional solvents [9–11].

For well-known reasons [12,13], gold particles are among the best-studied particles in materials science. There are also several examples of gold particle synthesis in ILs [14–18]. Like in classical synthesis protocols, reduction of Au(III) in ILs is often achieved with various reducing agents such as

NaBH₄. Moreover, it has recently been shown that the solubility of cellulose in ionic liquids [19,20] can be exploited for the synthesis of gold microcrystals [18].

The current study shows that injection of a mixture of HAuCl₄ and cellulose dissolved in the IL 1-butyl-3-methylimidazolium chloride, [Bmim]Cl, into aqueous NaBH₄ leads to gold nanoparticle/cellulose hybrids. The NaBH₄ rapidly reduces Au(III) to Au(0). At the same time, cellulose, which is soluble in [Bmim]Cl but not water, precipitates as fine nanofibers. The process is thus a model approach for the synthesis of (noble) metal/cellulose hybrids, which could find applications in sensing, sterile filtration, or biomaterials.

2. Results and Discussion

2.1. Results

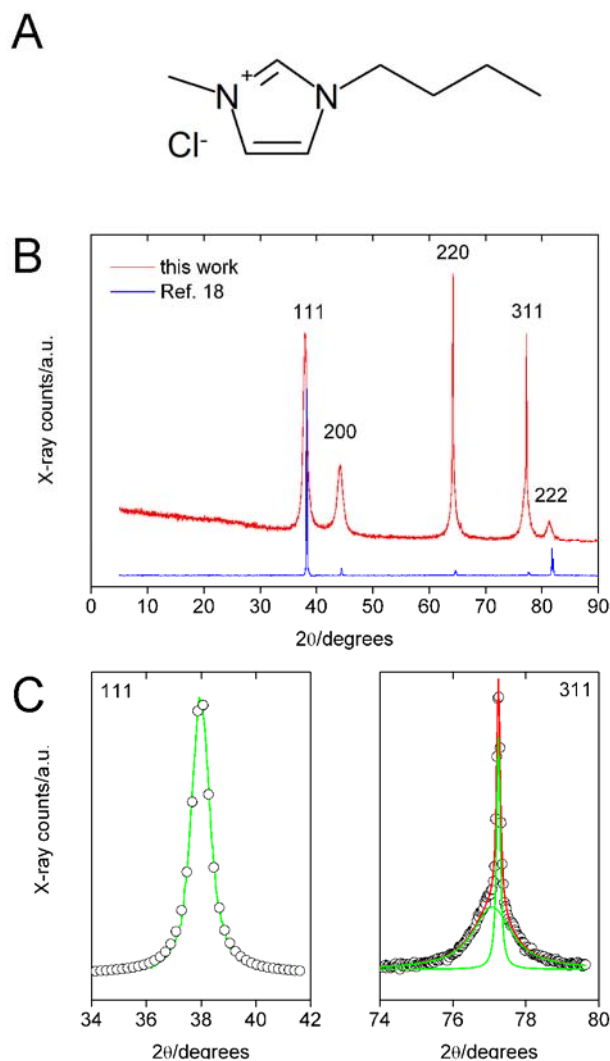
We have investigated the effects of gold and cellulose concentration. As neither of them has a strong effect on the structure of the resulting products, in the following we will focus on one main example, which was grown with 20 mg of HAuCl₄ and 20 mg of cellulose/g IL. The one effect that is important to control is the stirring time after injection. Immediate isolation of the products right after injection leads to poorly defined, unstructured materials (data not shown).

Figure 1 shows a typical X-ray diffraction (XRD) pattern of a gold nanoparticle/cellulose hybrid precipitate after isolation and drying. All products are pure face centered cubic (fcc) gold (JCPDS 04-0784). In most cases, the full widths at half maximum (FWHM) are larger than 1 degree 2 θ . The (110), (200), and (222) reflections can be fitted with a single Lorentzian. The (220) and (311) can only be fitted with a superposition of two Lorentzians. The crystallite sizes D_{hkl} (coherence lengths) calculated via the Scherrer equation [24] are in all cases around 10 nm. For the sample shown in Figure 1, D_{111} is 11.2, D_{200} is 6.6, D_{220} is 7.5, D_{311} is 7.8, and D_{222} is 7.1 nm. The reflections in XRD are thus much broader than those of samples grown in [Bmim]Cl, where cellulose acted as the reducing agent and the template for gold particle formation [18].

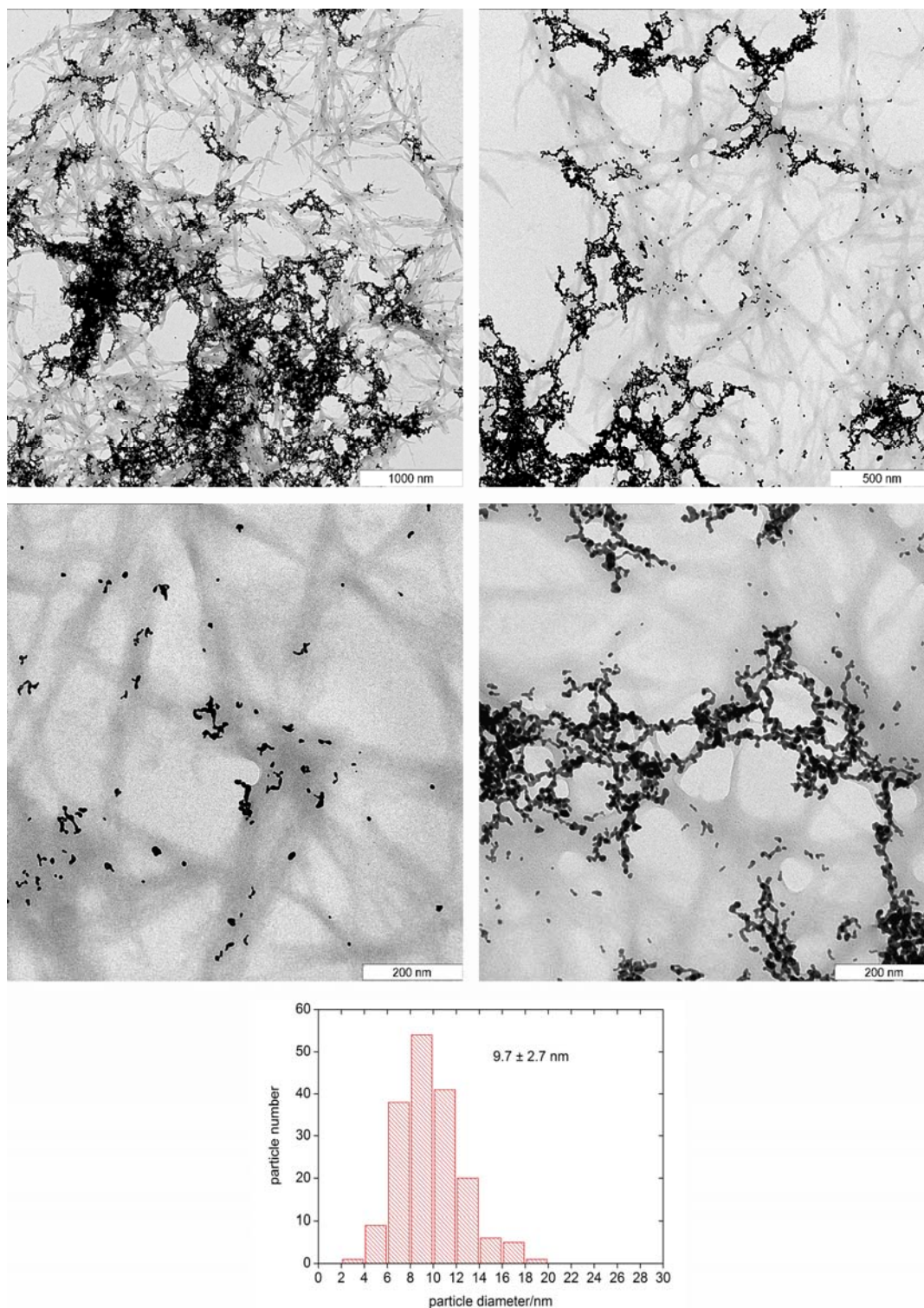
Although the synthesis process of the current material and the material described in ref. [18] is quite different, XRD shows no cellulose reflections in either case. The absence of cellulose reflections indicates that the cellulose, although precipitated, is only poorly crystalline. Possibly the NaBH₄ reducing agent not only reduces Au(III) to Au(0), but some reaction also takes place between the reducing agent and the cellulose.

Figure 2 shows representative transmission electron microscopy (TEM) images of the same precipitate. The cellulose fibers are short and only have a length of ca. one micron. The diameter distribution is rather broad and ranges from a few nm to tens of nm. As a result, TEM proves that not only gold nanoparticles, but also cellulose precipitates, even though no cellulose reflection appears in XRD. As the fibers are rather short, TEM supports the above hypothesis that, possibly, NaBH₄ also reacts with the cellulose. Partial degradation and poor order in the cellulose fibers due to rapid precipitation could also account for the fact that XRD does not detect cellulose reflections.

Figure 1. A: Structure of [Bmim]Cl. B: XRD pattern of a sample prepared via injecting a solution 20 mg of cellulose and 20 mg of $\text{HAuCl}_4 \cdot 3\text{H}_2\text{O}$ in 1 g of [Bmim]Cl into aqueous NaBH_4 . The pattern from ref. [18] is displayed for comparison. C: magnified (111) and (311) reflections showing the superposition of two Lorentzians for (311). Symbols are experimental data, green lines are individual Lorentzians, and red line is the superposition.



TEM further supports XRD, as both techniques observe gold particles with sizes below 20 nm. The D_{hkl} values from XRD agree well with the mean particle diameter of 9.7 ± 2.7 nm obtained from TEM. This suggests that the individual particles are single crystals, although TEM shows that they do not precipitate as single particles. Mostly, they form extended networks, similar to gold particles grown in polymer microgels [25,26]. The particles are exclusively observed on the cellulose fibers and individual gold wires follow the cellulose fibers. This suggests that the cellulose fibers act as scaffolds for nanoparticle growth or aggregation. The details of the process are currently under investigation.

Figure 2. TEM images and gold particle size distribution of the sample shown in Figure 1.

2.2. Discussion

The current paper shows that cellulose/gold(III) solutions in the IL [Bmim]Cl can be used for the fabrication of cellulose fiber/gold nanoparticle hybrid materials. The process is simple, robust, and fast and the resulting materials could be interesting for a variety of applications such as cellulose-supported gold nanoparticle sensors or for low temperature heterogeneous catalysts. The gold particles form

exclusively on the cellulose fibers and often, complex particle morphologies resembling earlier examples grown in polymer microgels [25,26], are observed in the TEM. XRD only shows signals from the gold and no cellulose reflections have been observed.

The absence of cellulose reflections indicates that the cellulose, although precipitated, is most likely only very poorly crystalline. It is also possible that the reducing agent used in this study, NaBH₄, not only reduces the Au(III) to Au(0) nanoparticles, but it is likely that some reaction also takes place between the reducing agent and the cellulose. This assumption is further supported by the observation of rather short cellulose fibers (around 1 μm in length), which is much shorter than what is usually observed in reconstituted cellulose.

Finally, as the IL is water soluble, there is only one liquid phase after injection of the IL solution into the aqueous phase. The cellulose/gold hybrid material precipitates and the IL, residual reducing agent, and the water form a homogeneous phase, which can easily be washed out. The aqueous phase after injection did not show any color, implying that the reduction reaction of the Au(III) to Au(0) is nearly quantitative.

3. Experimental

3.1. Synthesis

Cellulose (Acros, 10 to 100 mg) and H₂AuCl₄·3H₂O (Sigma, 10 to 100 mg) were mixed with [Bmim]Cl (Acros, 1 g). The mixture was heated to 100 °C until a clear solution formed. The solution was injected at room temperature into 0.2 M aqueous NaBH₄ (10 mL) under stirring, which was continued for 10 minutes. The precipitated products were recovered by repeated centrifugation, washed with water and ethanol and dried at 60 °C for 5 hours.

3.2. Characterization

X-ray diffraction (XRD) was done on a Nonius PDS 120 with a position sensitive detector (1 to 120 degrees 2θ) using CuKα radiation. Estimation of particle sizes was done as described previously [21–23]. After background subtraction, the peaks were fitted individually with Lorentzian profiles yielding the full width at half maximum (FWHM) and the x-centered position. The peaks were analyzed using the Scherrer formula [24]:

$$D_{hkl} = \frac{k * \lambda}{\beta * \left(\frac{\pi}{180}\right) * \cos \theta}$$

where D_{hkl} is the coherence length of the crystalline domain perpendicular to the respective hkl plane, k is a constant (here 0.9), λ is the wavelength of CuK_α radiation (1.5408 Å), β is the background-corrected line broadening in degrees, $(\pi/180)$ is a correction factor to calculate β in radians, and θ is the scattering angle. Transmission electron microscopy (TEM) was done on a LEO 912 Omega operated at 120 kV. Samples were suspended in ethanol and a drop of the suspension was directly deposited on carbon-coated copper grids. For comparison, samples were also studied without

centrifugation and washing. Image analysis was performed via AdobePhotoshop and OriginLab Origin 6.1.

4. Conclusions

In summary, we show that the unique ability of ILs to dissolve cellulose can be exploited for the fabrication of cellulose nanofiber/gold nanoparticle hybrids. The process is simple, robust, and fast and the resulting materials could be interesting for applications as cellulose-supported gold nanoparticle sensors or low temperature heterogeneous catalysts.

Acknowledgements

We thank R. Pitschke and H. Runge for help with electron microscopy, I. Zenke for help with XRD measurements, and the Swiss National Science Foundation, the MPI of Colloids and Interfaces, and the University of Potsdam for funding.

References and Notes

1. Endres, F.; El-Abedin, S.Z. Air and water stable ionic liquids in physical chemistry. *Phys. Chem. Chem. Phys.* **2006**, *8*, 2101–2116.
2. El-Abedin, S.Z.; Endres, F. Ionic liquids: The link to high-temperature molten salts. *Acc. Chem. Res.* **2007**, *40*, 1106–1113.
3. Reichert, W.M.; Holbrey, J.D.; Vigour, K.B.; Morgan, T.D.; Broker, G.A.; Rogers, R.D. Approaches to crystallization from ionic liquids: complex solvents–complex results, or, a strategy for controlled formation of new supramolecular architectures? *Chem. Commun.* **2006**, 4767.
4. Taubert, A. Inorganic materials synthesis—A bright future for ionic liquids. *Acta Chim. Slov.* **2005**, *52*, 183–186.
5. Taubert, A.; Li, Z. Inorganic materials from ionic liquids. *Dalton Trans.* **2007**, *7*, 723–727.
6. Parnham, E.R.; Morris, R.E. Ionothermal synthesis of zeolites, metal–organic frameworks, and inorganic–organic hybrids. *Acc. Chem. Res.* **2007**, *40*, 1005–1013.
7. Morris, R.E. Ionic liquids and microwaves-making zeolites for emerging applications. *Angew. Chem. Int. Ed.* **2008**, *47*, 442–444.
8. Li, Z.; Jia, Z.; Luan, Y.; Mu, T. Ionic liquids for synthesis of inorganic nanomaterials. *Curr. Opin. Solid State Mater. Sci.* **2008**, *12*, 1–8.
9. Nakashima, T.; Kimizuka, N. Interfacial synthesis of hollow TiO₂ microspheres in ionic liquids. *J. Am. Chem. Soc.* **2003**, *125*, 6386–6387.
10. Parnham, E.R.; Morris, R.E. Ionothermal synthesis using a hydrophobic ionic liquid as solvent in the preparation of a novel aluminophosphate chain structure. *J. Mater. Chem.* **2006**, *16*, 3682–3684.
11. Parnham, E.R.; Wheatley, P.S.; Morris, R.E. The ionothermal synthesis of SIZ-6—a layered aluminophosphate. *Chem. Commun.* **2006**, 380–382.
12. Daniel, M.C.; Astruc, D. Gold nanoparticles: assembly, supramolecular chemistry, quantum-size-related properties, and applications toward biology, catalysis, and nanotechnology. *Chem. Rev.* **2004**, *104*, 293–346.

13. Haruta, M. Gold as a novel catalyst in the 21st century: Preparation, working mechanisms and applications. *Gold Bull.* **2004**, *37*, 27–36.
14. Dobbs, W.; Suisse, J.M.; Douce, L.; Welter, R. Electrodeposition of silver particles and gold nanoparticles from ionic liquid-crystal precursors. *Angew. Chem. Int. Ed.* **2006**, *45*, 4179–4182.
15. Li, Z.; Liu, Z.; Zhang, J.; Han, B.; Du, J.; Gao, Y.; Jiang, T. Synthesis of single-crystal gold nanosheets of large size in ionic liquids. *J. Phys. Chem. B.* **2005**, *109*, 14445–14448.
16. Batra, D.; Seifert, S.; Varela, L.M.; Liu, A.C.Y.; Firestone, M.A. Solvent-mediated plasmon tuning in a gold-nanoparticle-poly (ionic liquid) composite. *Adv. Funct. Mater.* **2007**, *17*, 1279–1287.
17. Taubert, A.; Arbell, I.; Mecke, A.; Graf, P. Photoreduction of a crystalline Au(III) complex: a solid-state approach to metallic nanostructures. *Gold Bull.* **2006**, *39*, 205–211.
18. Li, Z.; Friedrich, A.; Taubert, A. Gold microcrystal synthesis via reduction of H₂AuCl₄ by cellulose in the ionic liquid 1-butyl-3-methyl imidazolium chloride. *J. Mater. Chem.* **2008**, *24*, 1008–1014.
19. Swatloski, R.P.; Spear, S.K.; Holbrey, J.D.; Rogers, R.D. Dissolution of cellulose with ionic liquids. *J. Am. Chem. Soc.* **2002**, *124*, 4974–4975.
20. Turner, M.B.; Spear, S.K.; Holbrey, J.D.; Rogers, R.D. Production of bioactive cellulose films reconstituted from ionic liquid. *Biomacromolecules* **2004**, *5*, 1379–1384.
21. Li, Z.; Shkilnyy, A.; Taubert, A. Room-temperature ZnO mesocrystal formation in the hydrated ionic liquid precursor (ILP) tetrabutylammonium hydroxide (TBAH). *Cryst. Growth Design* **2008**, *8*, 4526–4532.
22. Mumalo-Djokic, D.; Stern, W.B.; Taubert, A. Zinc oxide/carbohydrate hybrid materials via mineralization of starch and cellulose in the strongly hydrated ionic liquid tetrabutylammonium hydroxide. *Cryst. Growth Design* **2008**, *8*, 330–335.
23. Taubert, A.; Palms, D.; Glasser, G. Kinetics and particle formation mechanism of zinc oxide particles in polymer-controlled precipitation from aqueous solution. *Langmuir* **2002**, *18*, 4488–4494.
24. Guinier, A. *X-Ray Diffraction of Crystals, Imperfect Crystals and Amorphous Bodies*; Dover: New York, NY, USA, 1994.
25. Antonietti, M.; Gröhn, F.; Hartmann, J.; Bronstein, L.M. Nonclassical shapes of noble-metal colloids by synthesis in microgel nanoreactors. *Angew. Chem. Int. Ed. Engl.* **1997**, *36*, 2080–2083.
26. Roos, C.; Schmidt, M.; Ebenhoch, J.; Baumann, F.; Deubzer, B.; Weis, J. Design and synthesis of molecular reactors for the preparation of topologically trapped gold clusters. *Adv. Mater.* **1999**, *11*, 761–766.

Sample Availability: Samples of the hybrid materials are available from the authors on request.

© 2009 by the authors; licensee Molecular Diversity Preservation International, Basel, Switzerland. This article is an open-access article distributed under the terms and conditions of the Creative Commons Attribution license (<http://creativecommons.org/licenses/by/3.0/>).